Proceedings of the IASS 2024 Symposium
Redefining the Art of Structural Design
August 26-30, 2024, Zurich Switzerland
Philippe Block, Giulia Boller, Catherine DeWolf,
Jacqueline Pauli, Walter Kaufmann (eds.)

Fracture experiment of arch String Crescent Structure

Akira TANAKA*

* Associate Professor, Department of Industrial Information Tsukuba University of Technology, Japan
Amakubo 4-3-15, Tsukuba City, Ibaraki, 305-8520 Japan
Email akira@a.tsukuba-tech.ac.jp

Abstract

This study describes the results of fracture experiments on a unique masonry arch called String Crescent Structure (SCS). SCS consists of three components: Connect Members that prevent falling blocks, Lower String to form a stability arch, and Crescent Block with hollow. This block is made of thin shell elements, and block damage cannot be avoided, unlike conventional masonry structures. This damage leads to the falling blocks. To prevent this, Connect Members are installed between all blocks. Three types of models were created to simulate four hypothesized fracture modes. The fracture experiments were conducted by gradually applying a static load, and the fracture modes were observed. As a result, the Connect Members did not play a mechanical role under normal conditions, but they prevented the falling blocks at the time of fracture. Analysis was conducted, and the experiment and analysis values were compared.

Keywords: String Crescent Structure, Fracture experiment, Connect Member, Preferentially Broken Member, Support Condition, Fall Block

1. Introduction

In the 21st century, global warming and resource depletion have become huge issues, and various industries are developing technologies to promote the 3Rs (Recycle, Reuse, and Reduce). Conventional structures consume a significant amount of energy during production, construction, and demolition, which makes the development of new structural systems an urgent issue.

As one approach to addressing this challenge, Crescent Block that can be applied to various shaped structures was proposed. This block is a transformation of a wheel-like structure into a crescent shape, and is expected to satisfy the requirements of lightness, structural performance, and reusability (Fig. 1). The Crescent Block is composed of three parts: Rim, Hub, and Spoke. Rim is the block periphery and affects the overall structural performance of the block. Hub forms the structure by connecting the blocks. Spoke is radially arranged from Hub to Rim and improves the rigidity of Rim.

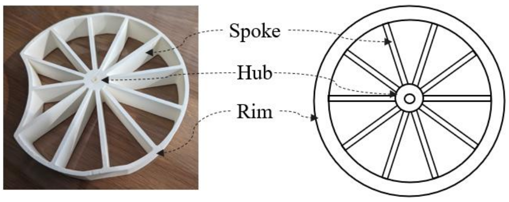

Figure 1: Crescent Block and Wheel

Connecting these blocks with Connect Members make a kinematic system that can be easily applied to various structural shapes. To stabilize this system, Lower Strings are installed, and the prestress is introduced. As a result, String Crescent Structure (SCS) is formed (Fig. 2). Applying this SCS to an arch form a unique masonry arch.

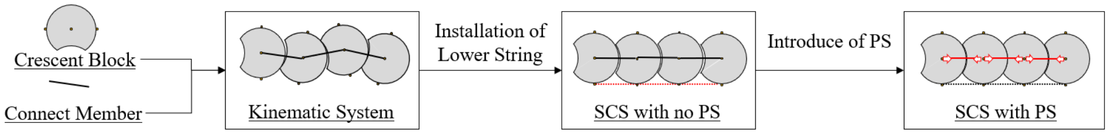

Figure 2: Formation of SCS

2. The subject of this research

SCS is a unique masonry arch proposed by the author. Therefore, there is very little prior research on it. [1] first proposed SCS and elucidated the structural characteristics and contact mechanism between blocks. In addition, [2] and [5] indicated that the prestress effect for arch-SCS reduce slippage and separation between blocks, improves bending rigidity, and lead to easy conduct analysis. However, stress was not reduced. Furthermore, [3] indicated that the friction coefficient of the blocks affects the stress state and stiffness, and [4] compared SCS with different support conditions and indicated that SCS with Pin-Pin support is more stable against cyclic load. However, the fracture mode of SCS has not been studied. This study aims to clarify the fracture mode of SCS. Specifically, the following three points will be clarified:

・Influence of different Support Conditions and the Lower String on the Fracture Mode of SCS,

・Role of Connector Member under fracture.

・Study of Analysis Model based on comparing experiment and analysis results of fracture.

The following four fracture modes were hypothesized based on the knowledge from previous experiments and analysis (Fig.3).

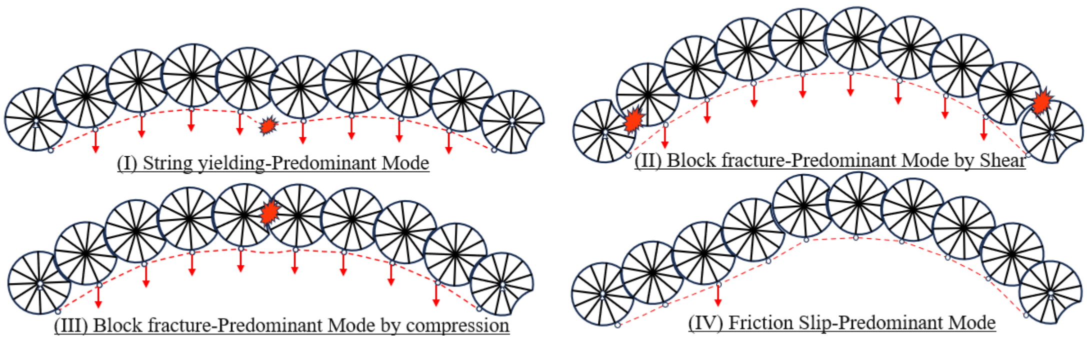

Figure 3: Assumptions of fractural mode in SCS

(I) String yielding-predominant mode When a moment works in SCS with pin-roller support, tension occurs in Lower Strings, and this will eventually yield-deformation. This condition occurs when the strength of Lower Strings is lower than that of the blocks.

(II) Block fracture-predominant Mode by Shear In SCS with pin-roller support, pressure lines and thrust do not form. As a result, separation and slipping easy occur between blocks. In addition, the blocks near the ends are destroyed.

(III) Block fracture-predominant Mode by Compression In SCS with pin-pin support, the thrust and a pressure line are formed within the arch. As a result, the blocks are destroyed by the bearing between the blocks. In the case of a pin-roller support, the occurrence condition is that the strength of the block is lower than that of Lower String.

(IV) Friction slip-predominant mode Blocks become unstable due to slipping or separation between blocks, leading to falling members. This facture mode is under a concentrated load. In addition, this mode can occur after any of the fracture modes (I), (II), and (III). This fracture mode is a dangerous phenomenon, and transition to this fracture mode should be prevented.

To study the aforementioned fracture modes, three types of models were created.

P-Type ; This was designed to simulate mode (III) and consisted of the low-strength Lower String and pin-pin supports.

BR-Type ; This was designed to simulate mode (II) or (III) and consisted of the high-strength Lower String and pin-roller supports.

SR-Type ; This was designed to simulate mode (I) and consisted of the low-strength Lower String and pin-roller supports.

Since the number of blocks for P-Type is large, a phenomenon similar to overall lateral buckling is expected to occur first, making it difficult to observe the destruction of the members. To avoid this, the number of blocks was limited to six. To prevent the falling blocks during fracture, Connect Members were installed in all models. However, the type without Connect Member is also used as the analysis model. Since there is a compression acting between the blocks, rigid members that can resist compression are suitable. In this study, the prestress isn't considered to reduce the factors that affect the fracture. The structural properties of Lower Strings for each model are shown in Table 2.

3. Tensile Test of Block Materials

Epoxy resin is the block material used. Its properties could be changed by the mixing environment, the type and amount of hardener and plasticizer. Increasing hardener ratio increases the hardness and brittleness. On the other hand, adding a plasticizer to the epoxy resin increases flexibility and elasticity. The epoxy for this experiment is a bisphenol-A epoxy resin. According to the catalog, the tensile strength was $70.6N/mm^2$, the compressive strength was $107.9N/mm^2$, and the flexural strength was $93.2N/mm^2$. However, the Young's modulus was not showed. Since the epoxy used in this study was prepared by myself, these catalog value and experimental value may differ. So, tensile test was conducted to evaluate the tensile properties of the specimens (Fig. 3). Tensile test methods are as follows. First, the spokes without large bubbles were cut out of the spare block (Fig. 3a). Then, a tensile test was conducted using an Instron tensile testing machine (Fig. 3b). The tensile speed was about $0.4mm/s$.

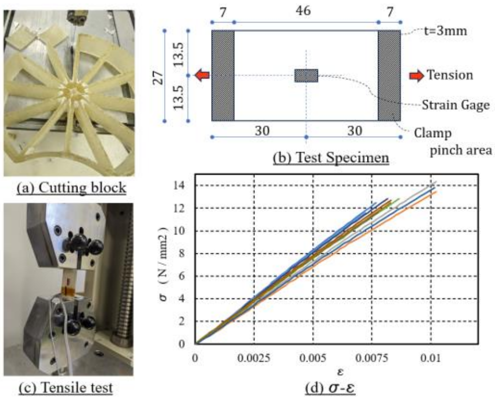

Figure 3: Tensile test of Block material

Table 1: Result of Tensile test

Number	Max. Tension (N)	ε_{max}	E_c (N/mm^2)
1	1090	0.0102	1286.02
2	1162	0.0102	1380.22
3	920	0.0076	1447.24
4	940	0.0072	1560.60
5	1040	0.0087	1447.24
6	1040	0.0082	1537.73
7	1030	0.0083	1493.90
8	940	0.0078	1447.84
9	1010	0.0083	1463.50
10	1120	0.0102	1332.57
11	1010	0.0077	1585.21

A series of 11 tensile tests revealed that all specimens exhibited brittle fracture before reaching the yield strength σ_y (Fig.3c). The tensile strength σ_t is equal to $13N/mm^2$, which is equivalent to the yield strength σ_y. The elastic modulus E_c was calculated from the strain ε under stress level $\sigma = 4N/mm^2$ ($Tension = 400N$), and the average value was $1450N/mm^2$. This value was input into the analysis model (Table 1).

4. Experiment and Analysis Models

4.1. Experiment Model

4.1.1. Structural specimen

The experiment model consists of (1) blocks with a diameter of 15cm, (2) Connect Members arranged on the neutral line, (3) Lower Strings, and (4) T-shaped Lower Joint. The rise-to-span ratio of the arch is 0.15, and is based on the arrangement shape of Connect Members (Fig. 4). The diameter of the bolt holes at both ends of Connect Members is designed to be large enough to allow a maximum gap of 3 mm between the bolts with a diameter of 3mm at the center of blocks. Because this loose bolt joint improves the mobility of Kinematic System.

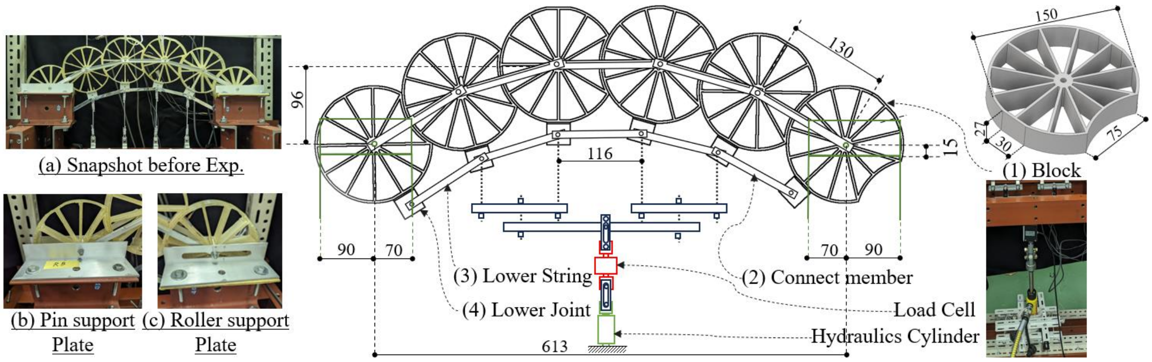

Figure 4: Experimental model

4.1.2. Measuring Point

Based on the results of a prior analysis, strain gauges for the blocks were set at points where damage was predicted. Specifically, for P-Type, the gauges were set near the center point. On the one hand, for BR and SR-Types, gauges were set near the ends (Fig. 5). Although displacement gauges were installed on each unit, the results near center point on the right are only shown this paper.

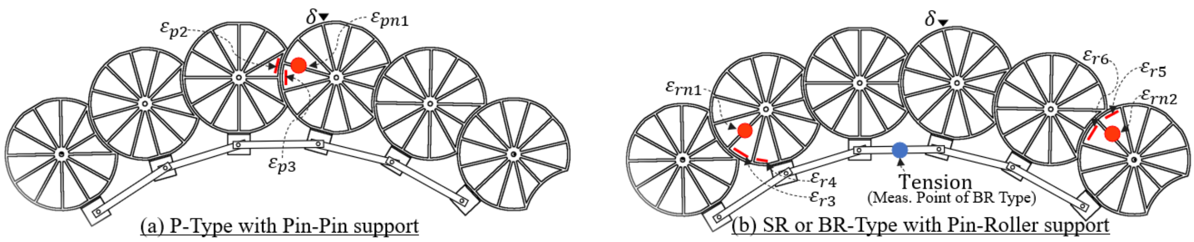

Figure 5: Meas. Points for Exp. or Analysis

4.1.3. Load Condition

The load was a four-point concentrated load applied by a manual hydraulic jack. The load experiment was conducted in two stages: the cyclic experiment and a fracture experiment. In this study, Prestress was not introduced, so there are micro-gaps between the blocks. As a result, there could be a large difference in the data between the analysis and experiment. Therefore, five cyclic loads ($\Sigma P = 50$ N) were conducted to reduce the gaps. After that, the fracture experiments for SCS were conducted.

4.2. Analysis model

The dimensions, boundaries, and loads of the analysis model are the same as those of the experiment model. The structural properties of SCS were studied using material nonlinear analysis with Inventor-Nastran. The analysis model current consists of blocks of solid elements and the line members of truss elements (Fig. 6).

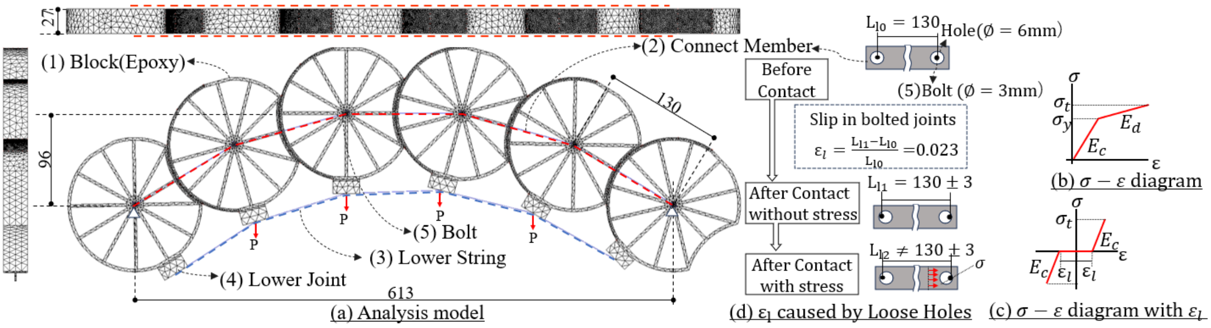

Figure 6: Analysis model

4.2.1. Detail of Members for Analysis models

The σ- ε diagrams for each member (Fig. 6(b)) were created based on the structural properties (Table 2). The considering the loose holes in Connect Member (Section 4.1.1), the σ- ε diagram for Connect Member is determined (Fig. 1(c)), and the value of ε_l was calculated following Fig. 1(d). The friction coefficient between the blocks was 0.2, based on the results of friction tests did several years ago [3].

Table 2: Structural variables

Name	Cross-Section (mm)	Material	Analysis Element (N , mm^2 or N/mm^2) Type	Area	Diagram	σ_y	σ_t	E_c	E_d	ε_s
(1)Block		Epoxy	Solid	−	Fig.6(b)	12	12	1480	0	−
(2)Connect Member	L − 10 × 10 × t1	AL	Truss	4.8	Fig.6(c)	310	375	68900	6450	0.023
(3)Lower String SP, SR	" 10 × t0.1 " × 2			2	Fig.6(b)	310	375	68900	6450	−
(3)Lower String BR	" 10 × t0.8 " × 2			16	Fig.6(b)	310	375	68900	6450	−
(4)Lower Joint	T − 30 × 30 × t2		Solid	−	Fig.6(b)	310	375	68900	6450	−
(5)Bolt	φ 3.0	Steel	Solid	−	Elasticity only	−	−	210000	−	−

4.2.2. Appropriate value of Contact Surface Mesh Size (α)

Inventor Nastran is suitable for contact analysis of planar elements. However, it can encounter errors when analysis curved surfaces. To address this issue, the contact surface mesh size (α) needs to be appropriately set. It is well-known that the mesh size of the continuum element affects the analysis precision. However, this relationship might not hold true for the contact surface, making it difficult to determine the optimal value of α. To solve this problem, four analysis models were created with varying block and support conditions. The blocks for these models were not only solid elements; a hybrid type (combining solid and shell elements) was also included for evaluation. The analysis results were obtained for different values of α, ranging from 0.5 to 5.5 mm (Fig. 7). Subsequently, the effect of α was compared between two models.

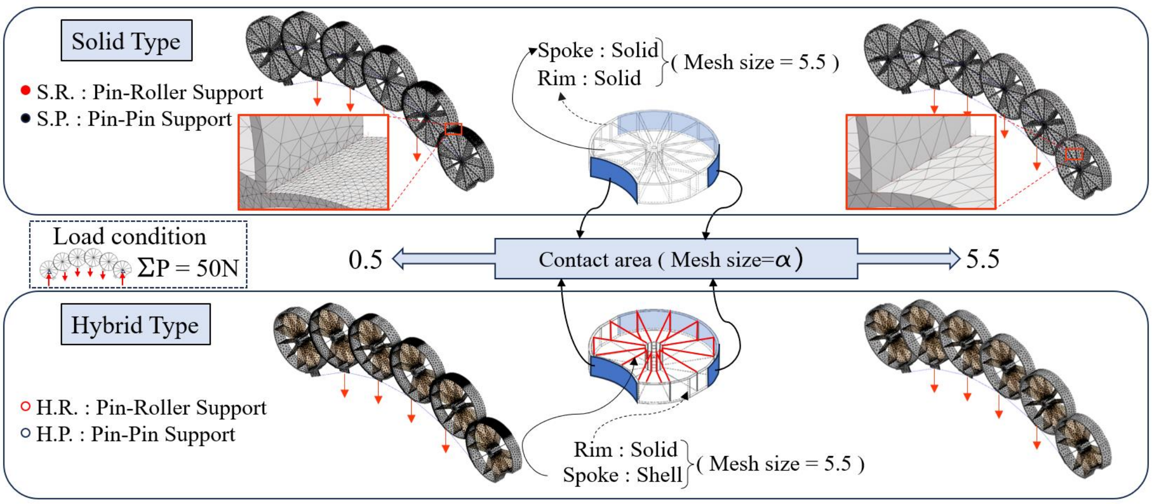

Figure 7: Solid and Hybrid Type for block

As the measurement point, one ε and one δ are chosen from those shown in Fig. 5. In the case of "S.P. and H.P.", ε_{p2} is chosen, and in the case of "S.R. and H.R. ", ε_{r5} is chosen.

Analysis was conducted while reducing difference in numerical value between "SP and HP" or "SR and HR". As a result, it was indicated that the optimal value of α is 1.0mm (Fig. 8). This α value was applied to the mesh size of the contact surface in the analysis model shown in Fig. 6.

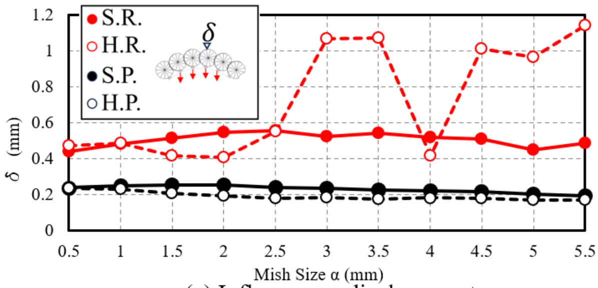

(a) Influence on displacement

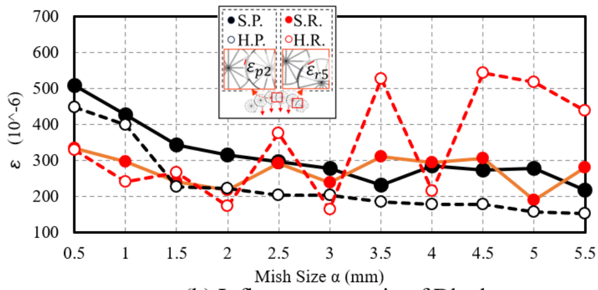

(b) Influence on strain of Block

Figure 8: Study on the optimal mesh size α for the contact area of blocks

The results for loads of $P \leq 50N$ are almost agreed between Hybrid models and Solid models, but different result is shown for loads exceeding $P = 50N$. Consequently, Hybrid models present reliability issues and will not be used for comparison with experiment models.

5. Results of experiment and analysis

5.1. P-Type

P-Type with pin-pin support was designed to operate in (III) mode (Fig. 3(III)). As predicted, brittle fracture of blocks occurred at the central point (Fig. 9(b)). When a block of a conventional masonry arch destructs, this structure becomes unstable and the blocks fall. However, in P-Type, Connector Members could support the damaged block after fracture, preventing the falling blocks and phenomenon like lateral buckling (Fig. 9(c)). When Connect Members supporting the damaged block were touched, it was confirmed that compression was acting, but those of the other units were wobbly. Although the total cross-sectional area of Lower Strings was extremely small at $2mm^2$, no yielding occurred. This suggests that the mechanical role of Lower Strings for P-Type is small.

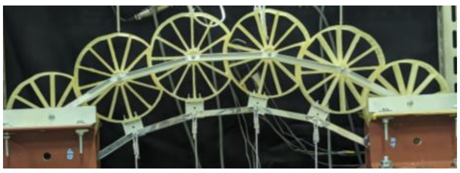

(a) Before Exp.

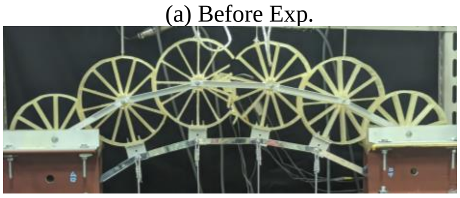

(b) After Exp.

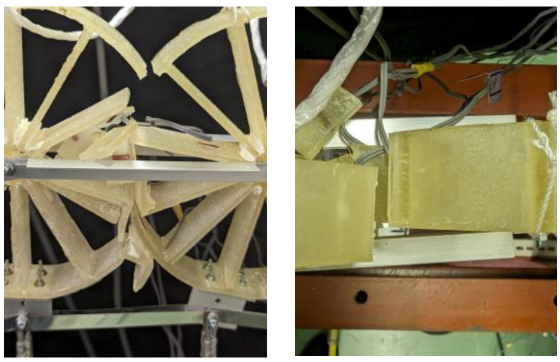

(c) Magnified view of the destruction

Figure 9: The snapshots of Exp. for P-Type

Although the maximum analysis load was 1100N, the experimental value was lower, at about 1000N (Fig. 10). The experiment model exhibited a larger displacement under low loads (Fig. 10a). This is caused by the gaps in the friction joints between blocks and the bolt joints of Low Strings. Additionally, the rapid displacement was observed in the experiment model under a load of 800 N. This is caused by the slipping between blocks. Other the one hand, the analysis model did not exhibit this phenomenon and showed a smooth P-δ curve. As a result of numerical comparison between experiment values and analysis values, the axial strain for spoke is larger, while the strain of rims is smaller. This indicates that rims are more prone to strain than spokes, which resist axial force.

Furthermore, the comparison between the two types of analysis models showed no differences in structural properties due to with or without Connect Members. This indicate that Connect Member with loose holes has no mechanical role in SCS before fracture.

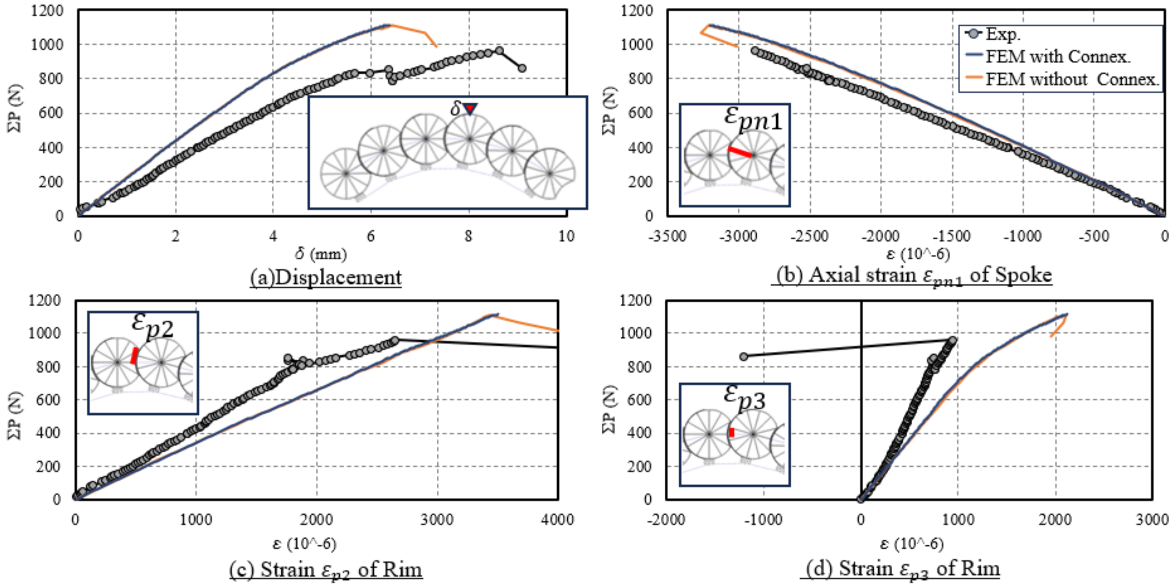

Figure 10: Structural behaviors of P-Type

5.2. SR-Type

SR-Type with pin-roller support was designed to operate in (I) mode (Fig. 3(I)). As expected, the central Low Strings of SR-Type were destroyed (Fig. 11). Like P-Type, Connect Members support damage block of SCS after fracture and prevents to fall the blocks.

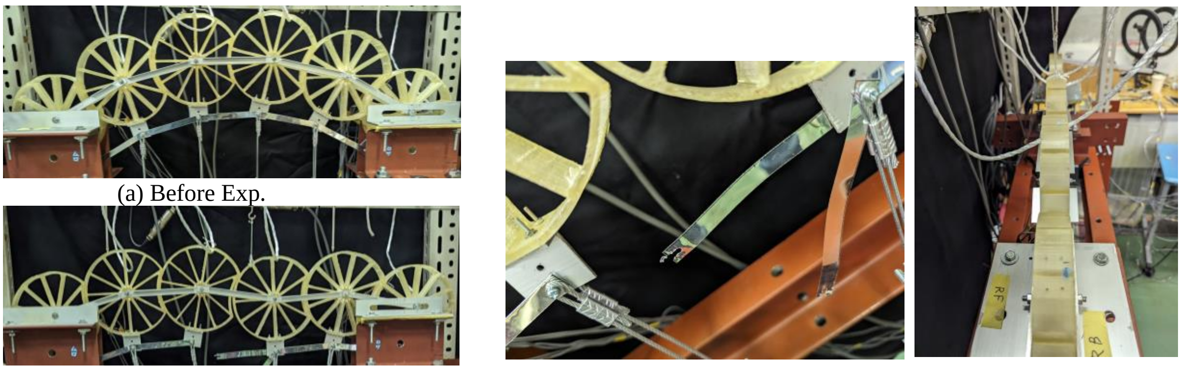

(a) Before Exp.

(b) After Exp.

(c) Magnified view of the destruction

Figure 11: The snapshots of Exp. for SR-Type

Although the analysis maximum load was 140 N, that of experimental value was much lower, about 60 N (Fig. 12). The reason for the difference between both of results is due to the reduced the durability of Lower String bolt joints caused by the accumulation of residual strain under cyclic load. A comparison of the results between analysis and experiments until reaching load of 50N shows that agreement in the axial strain of Spoke (Fig. 12(b)(c)), but poor agreement for Rim. This reason for this difference is the changing contact condition between the blocks caused by the cycle load. The results indicate that the influence of this change is greater for Rim than for Spoke. If the cyclic loading process is removed, will the difference between both of values become smaller? Based on the acknowledgements of past studies, it is estimated that prestress introduction is more effective than cyclic load to reduce the difference between experimental results and analysis results [1][2].

Furthermore, a comparison between the two types of analysis models showed no differences in structural properties with or without Connect Members.

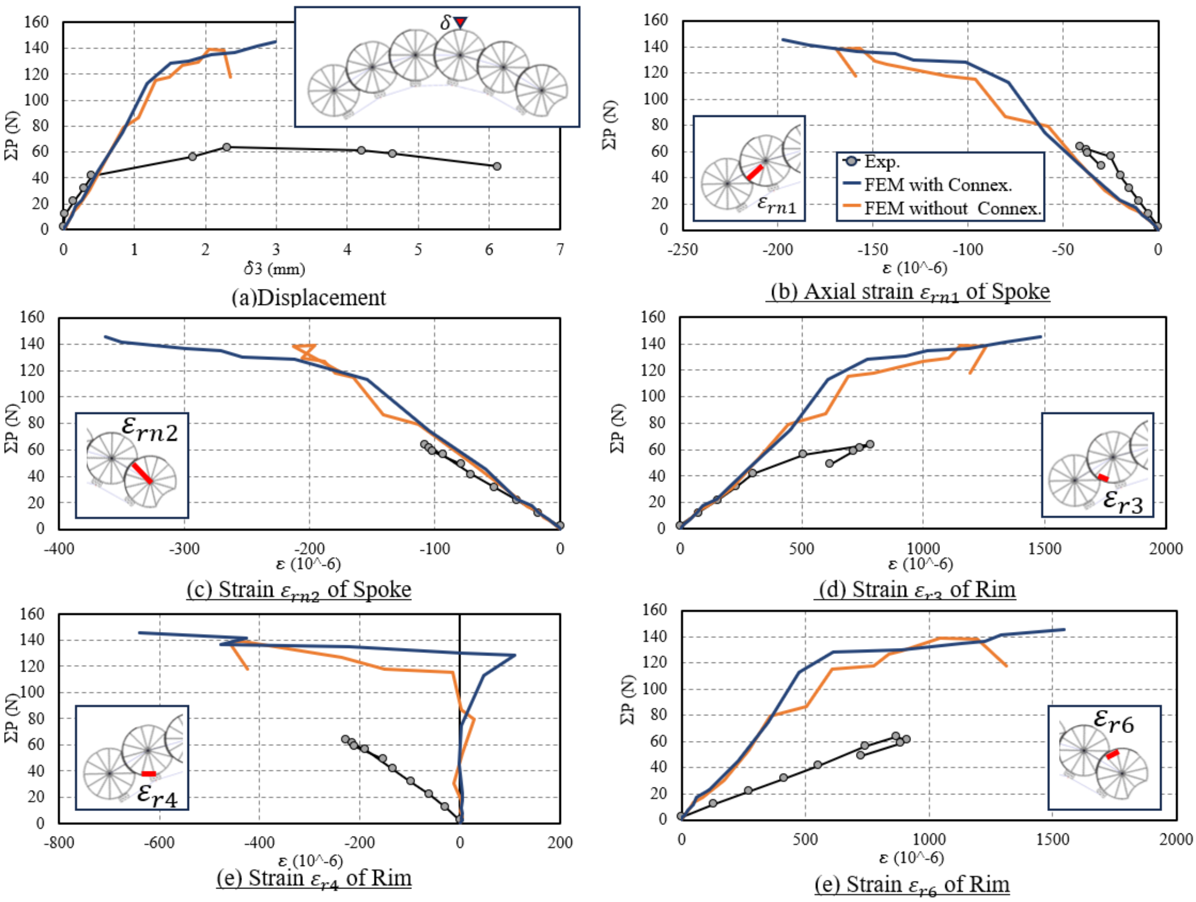

Figure 12: Structural behaviors of SR-Type

5.3. BR-Type

BR-Type with pin-roller support was designed to operate in (II) mode (Fig. 3(II)). At this time, it was predicted that the blocks near the end would be destroyed due to their separation and bearing. However, slipping between blocks occurred the right-end due to the tension of Lower String. As a result, the mechanical role of Lower String near the right-end was lost, and the adjacent block was pulled down by the load, and the tension spoke was damaged (Fig. 13). The state of Connect Members at this time was similar to the two types mentioned above too. However, there is a separation between the blocks during fracture. As a result, the tensile force acting on Connect Members supporting the damaging blocks (Fig. 13c).

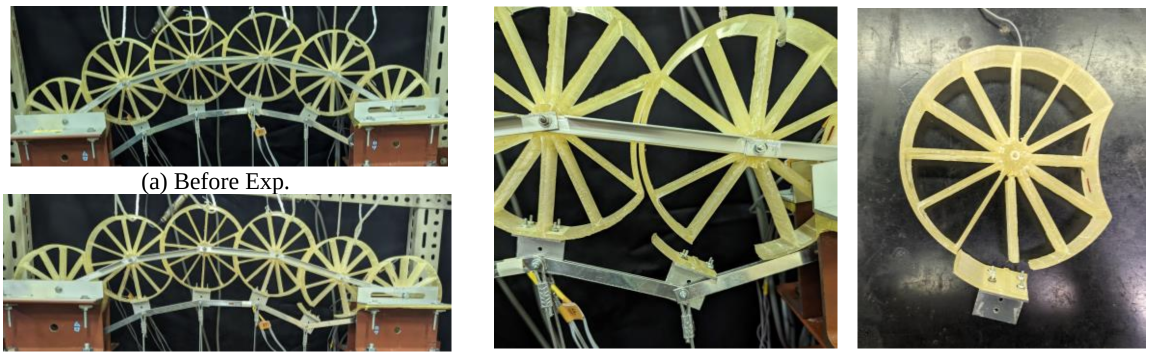
(a) Before Exp.
(b) After Exp.
(c) Magnified view of the destruction
Figure 13: The snapshots of Exp. for BR-Type

The maximum analysis load was about 600N. Other the one hand, the experiment result was about 720N (Figure 14). Rapid experimental values due to discontinuous slip was observed at measurement points on the left side of the experiment model (Fig. 14(b)(d)). In contrast, a smooth σ -

ε relationship due to continuous slip was observed on the right side (Fig. 14(c) (e)). The reason for difference in slip behavior between the two sides is the different contact condition of the blocks from near the left and right ends, and right end (Fig. 15(b)) has a condition that is easier slipping.

When comparing the amount of displacement, strain, and tension between the analysis and experiment, they did not agree. This tendency was especially evident in rim strain (Fig. 14(d)(e)). The reason for this is the same as that for SR-Type.

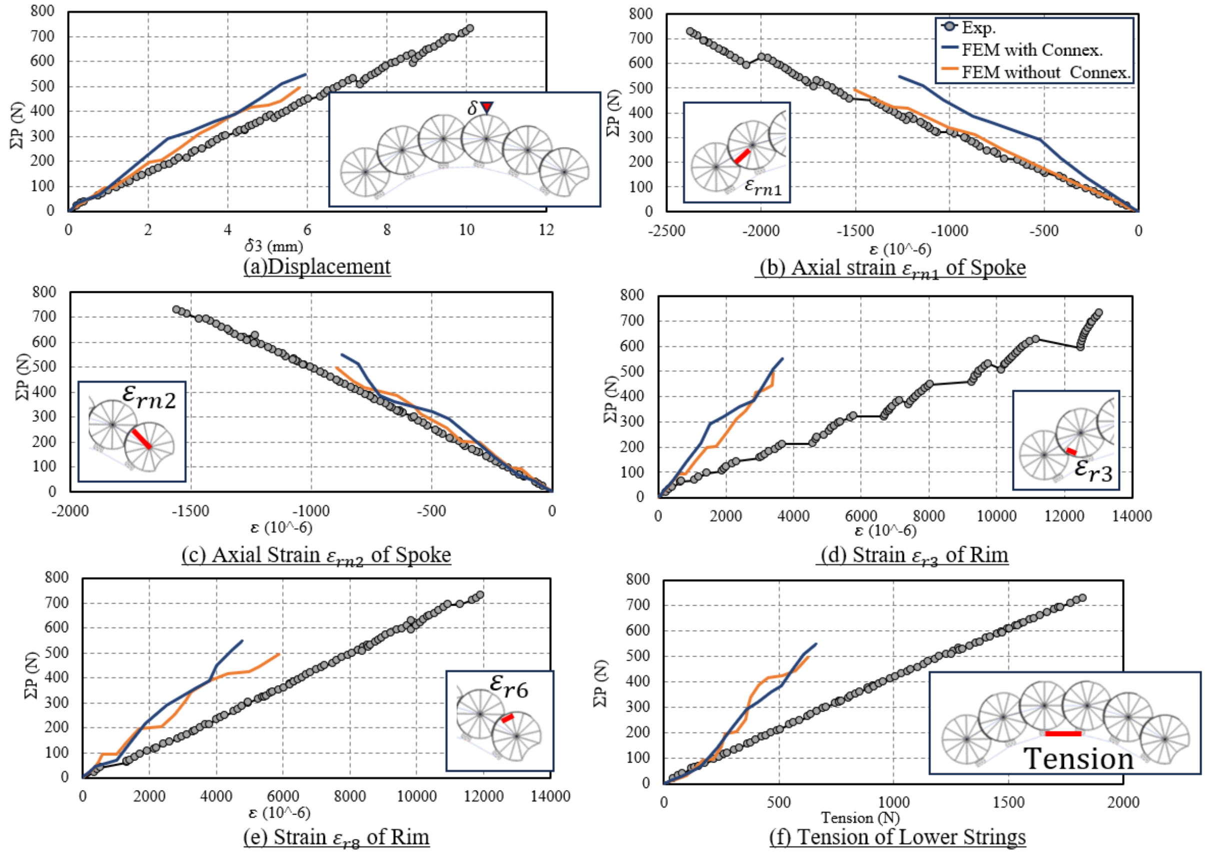

Figure 14: Structural behaviors of BR-Type

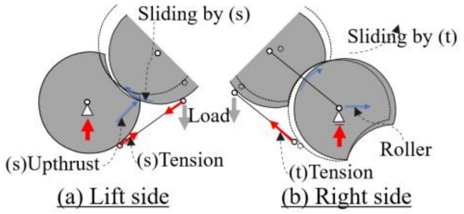

Figure 15: Structural behaviors of BR-Type

5.4. Reliability of analysis model

The analysis model with pin-roller support has many unstable elements that can cause slipping. As a result, the results are affected by various parameters of the nonlinear analysis (number of increments, arc length, set load level). On the other hand, since the model with pin-pin support has few unstable elements, the influence of these parameters is very small, and it is easy to create a highly reliable model.

Acknowledgements

The following knowledge was obtained from this study.

The fracture mode changes depending on the support conditions and the choice of stability members. In SCS with pin-pin support, compression occurs in the arch, and yielding damage occurs in the central blocks. In the case of pin-roller support, when Lower Strings are low-strength, a brittle fracture occurs in the central Lower String. When the Lower Strings are high-strength, spoke damage is induced by the slip between blocks near the end.

Connect Members act as supports for SCS after fracture, as confirmed by the experimental results. Regarding their role before fracture, the analysis shows that Connect Members have almost no effect.

There are some measurement points where the analysis results agree with the experiment results. However, in many other cases, there are large numerical differences in terms of maximum load and some strains. This undesirable outcome aligns with predictions from past studies. It is believed that introducing prestress into SCS could reduce this numerical difference [1, 2].

The challenges for future will be to verify the effect of prestress on fracture load and to develop a highly reliable analysis model.

References

[1] Akira TANAKA, *Proposal of String Crescent Structure - About concept and structural characteristic for String Crescent Structure* -, International Association for Shell and Spatial Structure (IASS2019), Barcelona, Spain.

[2] Akira TANAKA, *Load and Constructional Experiments on Beam-shape String Crescent Structure with Pretension Cables fitted to the neutral surface,* Proceeding of 12th Asian Pacific Conference on Shell & Spatial Structure (APCS2018), Penang, Malaysia

[3] Akira TANAKA, *The effect of friction coefficient of the structural behavior of String Crescent Structure,* International Association for Shell and Spatial Structure (IASS2021), Guilford, UK.

[4] Akira TANAKA, *The effect of changing boundary conditions at the arch End on the structural behavior of String Crescent Structure,* Proceedings of the IASS 2022 Symposium affiliated with APCS 2022 conference: Retractable Cable Tension Structures,Beijing,China, pp. 1-10(10)

[5] Akira TANAKA, *Structural behaviours of arch SCS with "pin-pin" support,* Proceedings of the International Association for Shell and Spatial Structure (IASS2023), Melbourne, Australia